24th INTERNATIONAL CONGRESS ON SOUND AND VIBRATION
23–27 July 2017, London

VIBRATION AND ACOUSTIC EMISSION MONITORING OF A GIRTH WELD DURING A RESONANCE FATIGUE TEST

Mohd Fairuz Shamsudin and Cristinel Mares

School of Engineering and Design, Brunel University, Uxbridge, Middlesex UB8 3PH, UK
email: mohd.fairuz.shamsudin@gmail.com

Carol Johnston, Graham Edwards and Tat-Hean Gan

TWI Ltd, Granta Park, Great Abington, Cambridge CB21 6AL, UK

This research is focused on LEVEL 1 detection and LEVEL 2 localization of damage which could be used as part of a structural health monitoring strategy. An experimental trial of acoustic emission and vibration monitoring techniques was carried out to monitor fatigue damage during a full scale resonance fatigue test on a girth welded pipe. The welded steel pipe was excited into the first mode of vibration using the resonance fatigue testing technique in order to determine the high cycle fatigue strength of the weld. The test applies a cyclic bending stress around the full pipe circumference at around 30Hz. The test was monitored in real time using acoustic emission and vibration monitoring. The damage sensitive features of the output from the vibration data were compared with the acoustic emission parameters. This paper shows that combining the vibration monitoring and acoustic emission results was effective since both techniques could detect damage from fatigue cracking in the extreme test conditions.
Keywords: acoustic emission, vibration monitoring, fatigue

1. Introduction

Vibration of piping and pipelines can cause fatigue damage and this is a problem for industry. A number of inspection techniques and monitoring systems are available however their application is not specific to addressing vibration induced fatigue in piping and pipelines. Guidelines have been published [1], in order to address piping vibration problems. These guidelines establish strategic assessment programs to identify immediate threats to piping systems and provide quantitative assessment to determine the risk of damage. This can be integrated further with vibration monitoring to quantify the integrity of piping systems.

Structural Health Monitoring (SHM) is the branch of reliability engineering with the main focus on evaluating structural condition by online monitoring. SHM is a strategic framework for detection of structural damage, localization, measuring damage extent and predicting the remaining life of structures [2]. A comprehensive review of SHM can be found in [3–6]. The general approach is that damage can be identified by vibration assessment i.e. damage can be inferred from the change of a structure's dynamic characteristics, such as measured system response (in the time domain and frequency domain), system mode shapes, modal damping and natural frequencies. However the change of dynamic characteristic may not be significant for structural failure due to localized damage such as cracks, which result in a negligible change of the overall structural stiffness. This can be problematic for vibration assessment of pressurized equipment such as piping or pipeline with potential loss of containment due to small cracks. An alternative approach is to identify the stress wave generated upon the onset of damage, which is known as a passive measurement technique. This is the fundamental principle of Acoustic Emission (AE), where stress waves generated by defects propagate within the structural domain and excite measurement sensors placed within their proximity.

2. Analysis and experimental procedures

Conventionally, AE techniques for damage assessment which are carried out are signal-based or parameter-based [7]. Signal-based analysis is a direct assessment where the transient signals recorded by acquisition systems are converted into frequency domain, time-frequency domain or by correlation methods [8–11]. The amount of acquired data can be prohibitively large which requires high computational power to condense large signals into meaningful results. The premise of using signal-based method is usually to obtain time of arrival for damage localization. It is important to note that the generated waves can be of many modes due to the interaction with geometrical boundaries. The waves have different velocities at different frequencies, exhibiting so-called 'dispersion' and in a plates such waves are called Lamb waves [12]. The identification of the arrival of waves is crucial, but correct source localization is complicated by dispersion. In general, high frequency waves suffer high attenuation and hence fundamental wave modes such as symmetric and anti-symmetric waves i.e. S0 and A0 respectively in plate-like geometry are usually obtained. However, waves in pipes have many additional modes which include the extensional, flexural and torsional modes.

The parameter-based is a classical approach which uses AE features for damage assessment. Commonly used features include: "count" (i.e. number of times AE signals cross the signal threshold), "burst energy" (i.e. the integral of squared acoustic emission signals over signal duration), or "burst signal rise time" (i.e. time difference between the first threshold crossing and peak amplitude) [13]. The parameter-based approach is used in many aspects of damage detection [14–17] and prognosis [18,19]. However it is highly dependent on threshold setting.

In this paper burst energy which is attributed to the rapid release of energy from damage and count were recorded for damage detection. The threshold setting was selected from a set of calibration measurements obtained by Pencil Lead Breakage (PLB) prior to the test to study wave attenuation and to determine the wave velocity.

In addition to high threshold setting, maximum arrival time limit, Δt_{max} is introduced by limiting the arrival time of subsequent sensors upon detection of signals by the trigger sensor. The trigger sensor is the first sensor that receives signal above threshold. Limiting the arrival time prevents the detection of AE signals reflected from features outside of the assessment area where the defect may present. However, this method requires certain arrangement of the sensors such that the defects are expected to be located in the circumcentre of a triangular sensor arrangement. The arrival time can then be mathematically calculated by;

$$\Delta t_{max} = \frac{\sqrt{(x - x_d)^2 + (y - y_d)^2}}{V_g} \tag{1}$$

where x_d, y_d are the defect locations, V_g is the group velocity, and x, y are the extent of the measurement area. This approach will remove further uncertainties of falsely detected AE signals, such as reflection from boundaries that may have larger arrival time beyond the arrival time limit.

For validation of AE signals, the strain history was recorded during fatigue loading. The premise of using strain history is that the change of strain rate or strain frequency such as frequency response of the structure under fatigue loading is associated with damage [20–22](Axial strain range was measured continuously during the fatigue test. However, the strain data is not presented in this paper to preserve confidentiality). Strain gauges can be an effective tool to measure vibration although they have some limiting factors [23–25]. Therefore, under normal condition without damage, the strain rate corresponds to the vibration frequency of the pipe. Damage causes the fluctuation of axial strain to increase and so the measured cycles obtained from the strain data. Therefore, the calculated cycles is higher compared with the actual cycles measured by an accelerometer and hence, gives indication of damage. The similarity and differences between AE features and strain measurement are discussed.

2.1 Experimental setup

A 15 inch diameter pipe with a 50mm wall thickness and made from carbon steel was used in this study. It was 7.2 m long and contained a girth weld at mid-length. The pipe was installed and tested in a resonance fatigue test machine [26]. During the test, the pipe was filled with water. This has the effect of increasing the overall mass and so reducing the pipe length as compared to the length theoretically required for the same resonant frequency in an empty pipe. The pipe length was chosen based on the mass of the pipe including internal medium and both end attachments to achieve pipe resonance in the first bending mode at around $30Hz$.

The resonance fatigue test rig comprises a drive unit at one end as shown in Figure 1-a. A 'balance' unit is present at the other end for symmetry. The drive unit contains an eccentric mass which provides a rotating eccentric force to the system when it is driven by a motor. The driving frequency was set to run the test at a particular strain range (as measured by strain gauges located at mid-length of the pipe). The pipe mid-section, where the welded joint is located, is subjected to the highest cyclic loading and hence highest cyclic stress resulting around the pipe circumference during the fatigue test. The stress varies from maximum and minimum with stress ratio R = - 1. This is superimposed on the axial stress generated by pressurising the water. The water pressure is chosen to produce an axial stress that is half of the applied stress range so that the resulting R ratio is greater than zero (R > 0). The pipe is supported at the nodes as illustrated in Figure 1-b where the displacement is negligible.

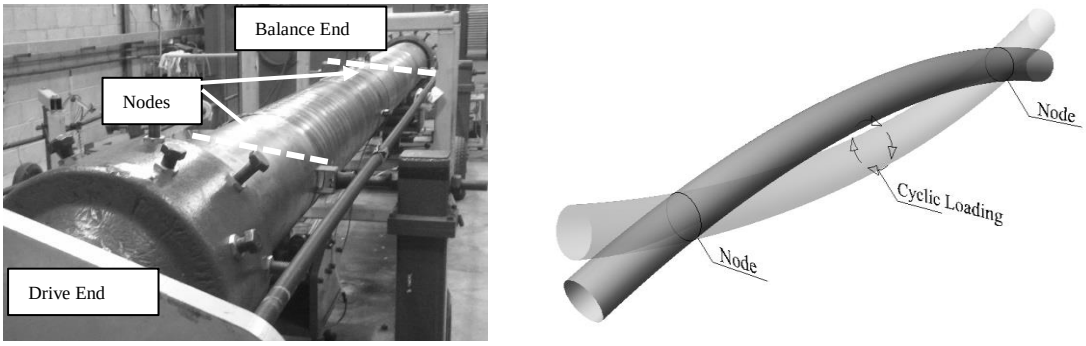

(a) (b)

Figure 1: The test set up. (a) Cyclic excitation is driven by a drive unit containing an eccentric mass at the drive end. There is a similar mass at the other (Balance) end for symmetry. (b) Two supporting systems are positioned at the nodes where the pipe displacement is negligible.

2.1.1 Instrumentation setup

Four broad band acoustic emission sensors model VS900-RIC with built in pre-amplifier propriety of Vallen Systeme were used with AMSY-6 multi-channels system. The system was set with $5MHz$ signal sampling rate and band-pass filter between $100kHz$ and $850kHz$. AE signals are highly contaminated by extraneous noise such as fretting at the pipe supports. Other sources of noise may be generated due to the mechanisms of fatigue cracking such as crack closure or crack face rubbing. Therefore, appropriate sensor positioning is crucial to avoid recording unwanted signals. In order to remove the effect of noise generated from the pipe supports itself and mechanical noise from both pipe ends, a guard sensor (i.e. the noises will hit the guard sensor before hitting the data sensors) was placed at 6 o'clock position at either side of the nodes close to the pipe supports.

The elastic deformation resulting from repetitive bending creates additional noise by friction between sensors and the pipe surface. To overcome this problem two sensors were located at each node where local displacement is negligible, as illustrated in Figure 2-a. The asymmetric sensor arrangement was such that two rings rotated by 90° against each other to avoid two possible locations exist if all sensors are on the same plane. This makes four combinations of isosceles triangular patterns i.e. 2-4-1, 4-1-3, 1-3-2 and 3-2-4 as illustrated in Figure 3. One aspect to consider using this triangular arrangement is that the circumcentre is not exactly coincident with the centre of the

height of isosceles triangle. This resulting in localization error if the weak point to be assessed is at the pipe mid-length between the nodes and hence need adjustment.

The vibration measurement was evaluated by the input and output signals. The input i.e. excitation frequency from the motor was closely monitored and compared against the output vibration response measured by an industrial accelerometer mounted near the weld joint. The measurement output was fed into the Vallen system as parametric input with sampling rate of $500Hz$.

The axial strain range was measured by eight equally spaced electrical resistance strain gauges mounted circumferentially. They were located 60mm from weld toe as shown in Figure 2-b. The strain gauges were high resistance quarter–bridge strain gauges with high excitation voltage. The measurement was sampled at $1kHz$ by National Instruments NI-9235 quarter bridge module configured in LabVIEW environment for post processing.

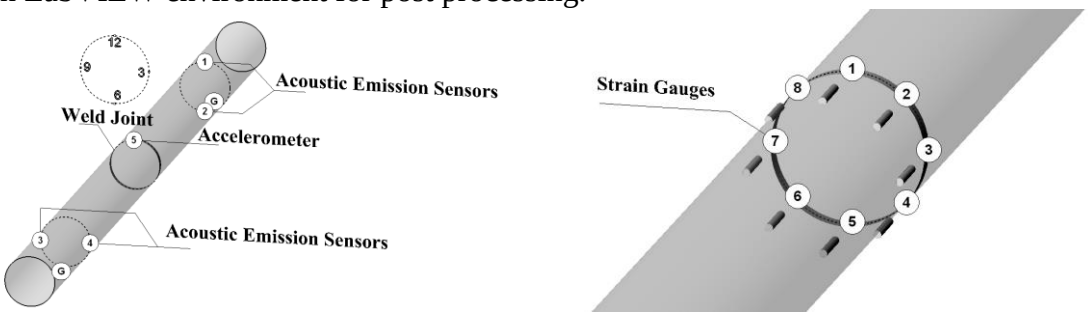

(a) (b)

Figure 2: (a) The location setup of AE sensors (numbered 1-4) at 12, 6, 9 and 3 o'clock positions respectively. A guard sensor (G) was mounted at 6 o'clock position close to each node and an accelerometer was mounted at 12 o'clock position in close proximity to the weld joint. (b) Eight equally spaced uniaxial strain gauges were attached 60mm from the weld joint.

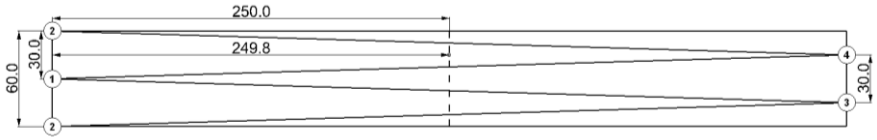

Figure 3: The combination of triangular patterns of sensor arrangement. Sensor 2 is labelled twice in each diagram which marks a complete pipe revolution. The dimensions shown are in centimetres.

2.1.2 Calibration measurement

A standard calibration measurement by PLB, which transmits the out of plane and in-plane waves from fractured lead, were conducted at the girth weld to examine whether AE signals were able to be detected by the AE sensors with the proposed sensor arrangement. The average group velocity, V_g was also determined by pulsing of AE sensors. It has been noted that using a single wave velocity can be erroneous due to the dispersion effect and mode conversion resulting from reflection from boundaries. The crack orientation could also influence the propagating waves [27]. In this work, the calculated velocity was assumed similar when the crack appears given that a high threshold setting was used to only capture the out-of-plane displacement i.e. dominant wave mode as crack propagates through thickness of the pipe. The calibration with PLBs was done at 3, 6, 9 and 12 o'clock positions. The calculated velocity was $3000m/s$ at 70dB threshold setting.

The propagated waves were identified by comparing the wave velocity against DISPERSE code [28] (i.e. a general purpose program for crating dispersion curves). The frequencies of the arrival waves were approximately $180kHz$. From the dispersion curves, a number of wave modes exist at the measured frequency however, the waves travel at the measured velocity consist of L(0,1), L(0,2), F(1,1) and F(1,3) as shown in Figure 4-a. The mode shapes corresponding to these waves are illustrated in Figure 4-b.

3. Results and discussion

The resonance test lasted in this experiment from start-up to failure for six days (corresponding to 14,106,360 applied cycles). The driving motor was immediately stopped by a trip system as soon as the internal pressure in the pipe dropped rapidly resulting from loss of containment due to through-wall cracking. The failure location was identified at 6 o'clock position where a 4mm crack length was present on the pipe outer wall. The crack had initiated on the inner surface and propagated through the pipe thickness.

During the test, there were burst-like signals associated with cracks as illustrated in Figure 5-a. The burst signals consist of a number of wave trains. Signals associated with noise were also recorded despite high threshold setting used as shown in Figure 5-b. These signals may correspond to plastic deformation [29,30], crack face rubbing as a result of different crack modes and other sources of extraneous noises which are unknown.

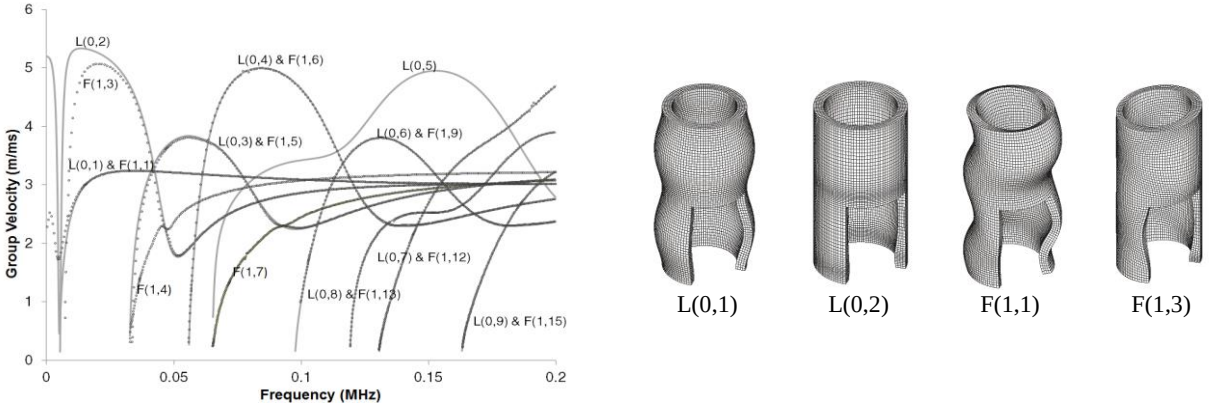

(a) (b)

Figure 4: (a) The dispersion curves of the steel pipe calculated by DISPERSE code. The continuous lines are the extensional modes and dotted lines are the flexural modes. (b) The mode shapes of the extensional L(*n*,*m*) and flexural F(*n*,*m*). The *n* and *m* are the circumferential and axial nodal patterns respectively [31]

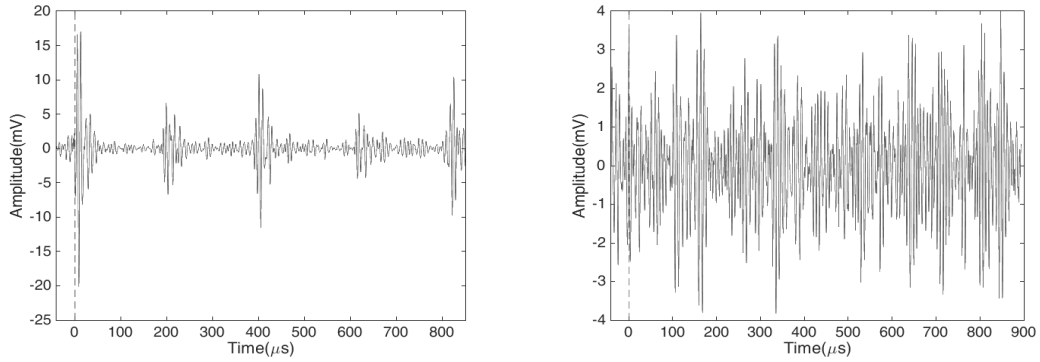

(a) (b)

Figure 5: Example of AE signals (a) due to cracking (b) and noise.

AE count and energy were plotted to observe the propagating damage. There were several peaks recorded by the AE energy as is illustrated in Figure 6-a. These peaks may correspond to the evolution of damage. The time interval of 30s was selected where each AE feature i.e. count and energy were cumulatively calculated. The results from the strain records and vibration monitoring ;by calculating the number of cycles recorded by the accelerometer i.e. actual cycles, N_a, divided by the number of cycles recorded from the strain data, N_s, as illustrated in Figure 6-b, were compared with the AE features.

The parametric data from vibration was extracted and Short Time Fourier Transform (STFT) with low-pass filter was calculated at the marked points (Point 1–8) to observe whether any frequency change would appear in the event of damage. The STFT was also calculated for one hour

duration at the beginning and at the end of the test. The vibration frequencies at the marked points were consistently calculated to be 30*Hz* which showed that the excitation frequency of the pipe remained constant throughout the test, and is equivalent to the resonance frequency. However, the vibration amplitudes increased considerably towards the end as shown in Figure 7.

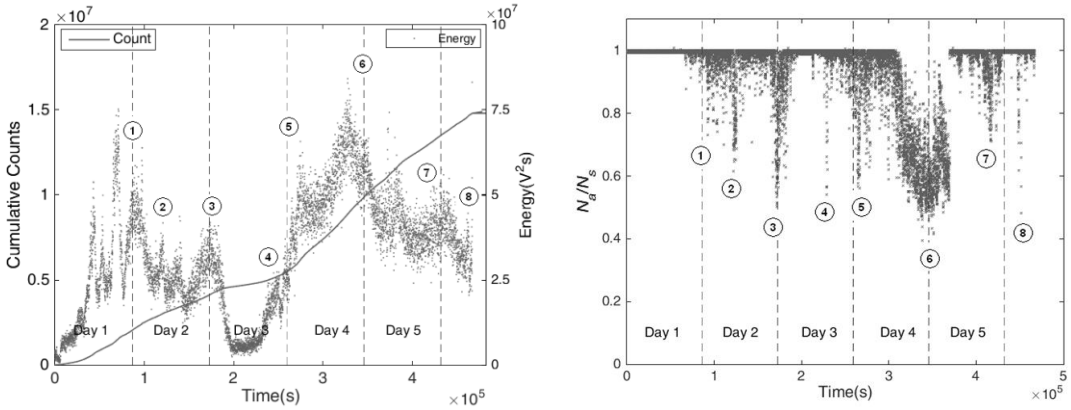

(a) (b)

Figure 6: (a) Acoustic emission features i.e. energy and count extracted from the AE signals (b) and the ratio of actual number of cycles to the calculated cycles from strain fluctuation

The axial strain rate varies according to the resonance frequency towards the end of day 1 (point 1) before the strain starts to fluctuate. Prior to this event, a number of sharp rises and falls of AE energy were observed which is believed to be associated with micro-fracture phases [32].

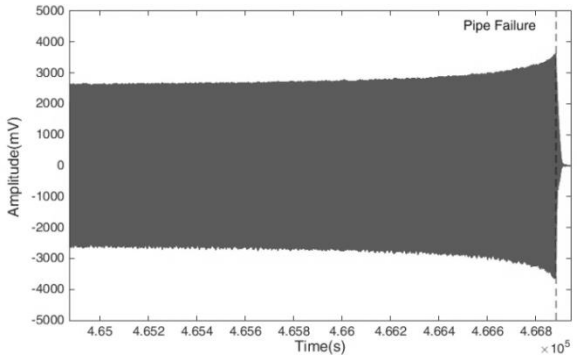

Figure 7: vibration signal recorded by the accelerometer.

The AE energy continues to accumulate which may results from continuous emission of plastic deformation, crack initiation, deformation twinning, or phase transformation [30,33,34] at points 2 and 3. In this test specimen, it is most likely to be due to crack initiation. Similar trend was observed by the strain fluctuation, thus increases the number cycles calculated by the strain measurement which leads to the reduction of the ratio *Na/Ns* as shown in Figure 6-b. However, between points 3 and 4, the AE energy decreases suddenly to the minimum level which implies the noise threshold level in the system. During this period the cracks have stopped propagating and no located event was identified.

The AE energy starts to increase tremendously between points 4 and 6 and recorded the highest peak. At these intervals the signals have longer duration which is associated with rapid releases of energy from crack activities. The longer duration and high amplitude signals result in the increase of AE count. Similar trend can be observed from the strain data where the number of measured cycles increased considerably at point 6 upon large crack growth at a number of located events as illustrated in Figure 8. The crack growth was concentrated at localised areas particularly at 12 o'clock and 6 o'clock which suggest active weak points. The severity of damage from the high density of located events means potential failure at this location is imminent. However the AE energy started to decay where smaller recorded peaks after point 6 and immediately before failure i.e. point 8. The reduction in energy means fewer short duration signals exceeding the threshold. This implies

the out-of-plane waves, which have smaller magnitude, dominate when the crack propagated through thickness and the crack length increases [35].

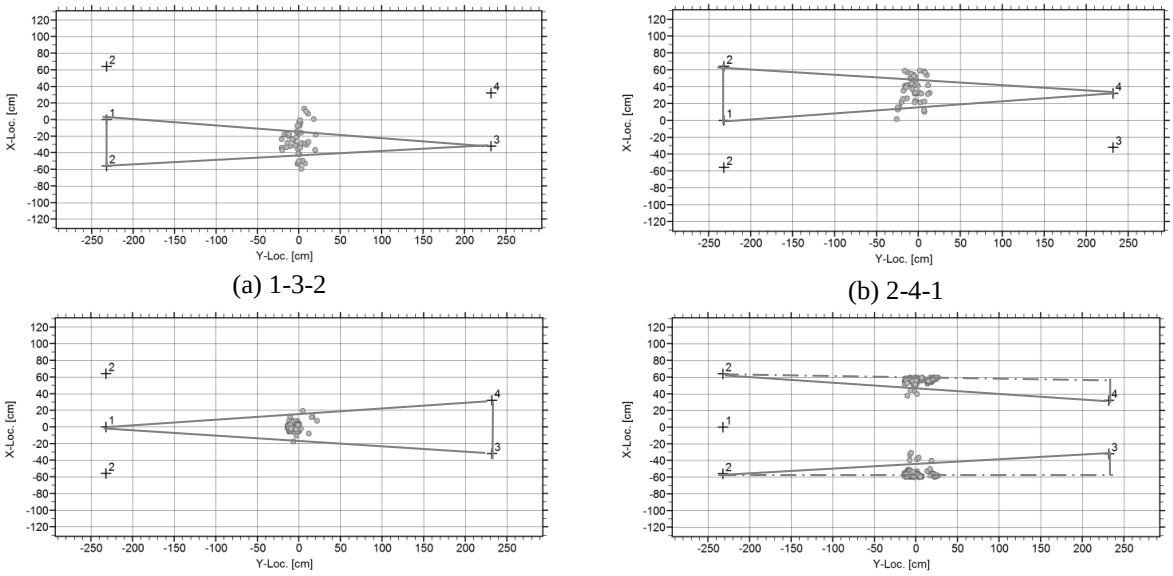

(a) 1-3-2 (b) 2-4-1

(c) 4-1-3 (d) 3-2-4

Figure 8: The located events when the pipe failed

4. Summary and conclusions

The aim of this paper is to demonstrate the application of Acoustic Emission (AE) and vibration methods in monitoring pipe condition. A pipe was excited continuously by means of a resonance fatigue testing machine to evaluate the integrity of a girth weld subjected to fatigue loading. The calculated cycles from the recorded strain data and vibration monitoring provide damage sensitive features which were found to be consistent with the AE measurement. Integration of the techniques provides important information about the condition of the pipe throughout the test. The usage of the maximum arrival time limit, Δt_{max} and high threshold setting eliminated significant background noises and hence making the AE monitoring feasible. However, prior understanding of the type of the waves when AE signals are recorded is crucial which, in this study, was determined by a set of calibration by Pencil Lead Breakage. A large number of events concentrated at 12 o'clock and 6 o'clock positions which indicate the potential failure locations with a proper sensor arrangement for effective localization method. A study on signal processing techniques for discriminating the noises will be carried out as the future work using current experimental data.

5. Acknowledgement

This publication was made possible by the sponsorship and support of Fatigue Integrated Management and Condition & Structural Monitoring sections at TWI, Brunel University London, and Majlis Amanah Rakyat (MARA). The work was enabled through, and undertaken at, the National Structural Integrity Research Centre (NSIRC).

REFERENCES

1 Energy Institute, "Guidelines of the Avoidance of Vibration Induced Fatigue Failure in Process Pipework," Second edition,(2003).

2 A. Rytter, *Vibrational Based Inspection of Civil Engineering Structures*, Ph. D. Dissertation, Department of Building Technology and Structural Engineering, Aalborg University, Denmark, (1993).

3 E. P. Carden and P. Fanning, "Vibration based condition monitoring: a review," *Structural health monitoring*, vol. **3**, no. 4, pp. 355–377, (2004).

4 S. W. Doebling, C. R. Farrar, M. B. Prime, and D. W. Shevits, "A summary review of vibration-based damage identification methods," *Shock and vibration digest*, vol. **30**, no. 2, pp. 91–105, (1998).

5 W. Fan and P. Qiao, "Vibration-based damage identification methods: a review and comparative study," *Structural Health Monitoring*, vol. **10**, no. 1, pp. 83–111, (2011).
6 H. Sohn, C. R. Farrar, F. M. Hemez, D. D. Shunk, D. W. Stinemates, B. R. Nadler, and J. J. Czarnecki, A review of structural health monitoring literature: 1996-2001. Los Alamos National Laboratory Los Alamos, NM,(2004).
7 C. U. Grosse, H. W. Reinhardt, and F. Finck, "Signal-based acoustic emission techniques in civil engineering," *Journal of materials in civil engineering*, vol. **15**, no. 3, pp. 274–279, (2003).
8 G. Curtis, "Acoustic emission-4: Spectral analysis of acoustic emission," *Non-Destructive Testing*, vol. **7**, (1974).
9 D. Masera, P. Bocca, and A. Grazzini, "Frequency analysis of acoustic emission signal to monitor damage evolution in masonry structures," in *Journal of Physics: Conference Series*, (2011), vol. **305**, no. 1, p. 012134.
10 A. C. Okafor, K. Chandrashekhara, and Y. Jiang, "Location of impact in composite plates using waveform-based acoustic emission and Gaussian cross-correlation techniques," in *Symposium on Smart Structures and Materials*, (1996), pp. 291–302.
11 W. Prosser, M. D. Seale, and B. T. Smith, "Time-frequency analysis of the dispersion of Lamb modes," *The Journal of the Acoustical Society of America*, vol. **105**, no. 5, pp. 2669–2676, (1999).
12 H. Lamb, "On waves in an elastic plate," *Proceedings of the Royal Society of London. Series A, Containing papers of a mathematical and physical character*, pp. 114–128, (1917).
13 Non-destructive testing. Terminology. Terms used in acoustic emission testing. BS EN 1330-9:2009, (2009).
14 M. Bassim, "Detection of fatigue crack propagation with acoustic emission," *NDT & E International*, vol. **25**, no. 6, pp. 287–289, (1992).
15 M. Bassim, S. S. Lawrence, and C. Liu, "Detection of the onset of fatigue crack growth in rail steels using acoustic emission," *Engineering Fracture Mechanics*, vol. **47**, no. 2, pp. 207–214, (1994).
16 W. H. Prosser, "Advanced AE techniques in composite materials research," *Journal of Acoustic Emission*, Vol **14**, pp. S1-S11 (1996).
17 P. Vanniamparambil, U. Guclu, and A. Kontsos, "Identification of crack initiation in aluminum alloys using acoustic emission," *Experimental Mechanics*, vol. **55**, no. 5, pp. 837–850,(2015).
18 A. Carpinteri, G. Lacidogna, and N. Pugno, "Structural damage diagnosis and life-time assessment by acoustic emission monitoring," *Engineering Fracture Mechanics*, vol. **74**, no. 1, pp. 273–289, (2007).
19 B. A. Zárate, J. M. Caicedo, J. Yu, and P. Ziehl, "Probabilistic prognosis of fatigue crack growth using acoustic emission data," *Journal of Engineering Mechanics*, vol. **138**, no. 9, pp. 1101–1111, (2012).
20 Y. Murakami, "Recorder and application to fatigue design of car wheels," *Fatigue Design and Reliability*, vol. **23**, p. 135, (1999).
21 A. S. J. Swamidas and Y. Chen, "Monitoring crack growth through change of modal parameters," *Journal of Sound and Vibration*, vol. **186**, pp. 325–343, (1995).
22 A. S. J. S. Yin Chen, "Change of modal parameters due to crack growth in a tripod tower platform," *Canadian Journal of Civil Engineering*, vol. **20**, pp. 801–813, (1993).
23 G. Pavi, "Measurement of vibrations by strain gauges, part I: theoretical basis," *Journal of Sound and vibration*, vol. **102**, no. 2, pp. 153–163, (1985).
24 G. Pavi, "Measurement of vibrations by strain gauges, part II: selection of measurement parameters," *Journal of Sound and Vibration*, vol. **102**, no. 2, pp. 165–188, (1985).
25 E. J. Wilson, "Strain-gage Instrumentation," *Harris' Shock and Vibration Handbook*, 2nd ed, McGraw-Hill Book Company, New York, (1976) , Chap. 13.
26 Y.-H. Zhang and S. Maddox, "Development of fatigue testing of full-scale girth welded pipes under variable amplitude loading," *ASME 2011 30th International Conference on Ocean, Offshore and Arctic Engineering*, (2011).
27 M. R. Gorman and W. H. Prosser, "AE source orientation by plate wave analysis," *J. Acoust. Soc. Am.* ***90*** (1991).
28 B. P. Michael Lowe, DISPERSE, 2.0.20a ed. Non-Destructive Testing Laboratory, Department of Mechanical Engineering, Imperial Colleage London, (2013).
29 K. ONO, H. CHO, and M. Takuma, "The origin of continuous emissions," *Journal of Acoustic Emission*, vol. **23**, p. 206, (2005).
30 A. Rao, "Acoustic emission and signal analysis," *Defence Science Journal*, vol. **40**, no. 1, p. 55, (1990).
31 S. Sorohan, N. Constantin, M. Găvan, and V. Anghel, "Extraction of dispersion curves for waves propagating in free complex waveguides by standard finite element codes," *Ultrasonics*, vol. **51**, pp. 503–515, (2011).
32 M. R. Kaphle, A. Tan, D. Thambiratnam, and T. H. Chan, "Damage quantification techniques in acoustic emission monitoring," *WCEAM 2011 Sixth World Congress onEngineering Asset Management*, (2011).
33 C. Heiple and S. Carpenter, "Acoustic emission produced by deformation of metals and alloys-A review.," *Journal of Acoustic Emission*, vol. **6**, pp. 177–204, (1987).
34 M. Huang, L. Jiang, P. K. Liaw, C. R. Brooks, R. Seeley, and D. L. Klarstrom, "Using acoustic emission in fatigue and fracture materials research," *JOM 50.11*, vol. **1–14**, (1998).
35 C. Lee, J. J. Scholey, P. D. Wilcox, M. Wisnom, M. I. Friswell, and B. Drinkwater, "Guided wave acoustic emission from fatigue crack growth in aluminium plate," in *Advanced Materials Research*, (2006), vol. **13**, pp. 23–28.